Site symmetry dependence of repulsive interactions between chemisorbed oxygen atoms on Pt{100}-(1×1)

Q. Ge, P. Hu,[a)] and D. A. King
Department of Chemistry, Lensfield Road, Cambridge CB2 1EW, United Kingdom

M.-H. Lee,[b)] J. A. White, and M. C. Payne
Cavendish Laboratory, Madingley Road, Cambridge CB3 0HE, United Kingdom

Ab initio total energy calculations using density functional theory with the generalized gradient approximation have been performed for the chemisorption of oxygen atoms on a Pt{100}-(1×1) slab. Binding energies for the adsorption of oxygen on different high-symmetry sites are presented. The bridge site is the most stable at a coverage of 0.5 ML, followed by the fourfold hollow site. The atop site is the least stable. This finding is rationalized by analyzing the ''local structures'' formed upon oxygen chemisorption. The binding energies and heats of adsorption at different oxygen coverages show that pairwise repulsive interactions are considerably stronger between oxygen atoms occupying fourfold sites than those occupying bridge sites. Analysis of the partial charge densities associated with Bloch states demonstrates that the O–Pt bond is considerably more localized at the bridge site. These effects cause a sharp drop in the heats of adsorption for oxygen on hollow sites when the coverage is increased from 0.25 to 0.5 ML. Mixing between oxygen *p* orbitals and Pt *d* orbitals can be observed over the whole metal *d*-band energy range. [S0021-9606(97)00303-6]

I. INTRODUCTION

CO oxidation may be considered as a prototype surface chemical reaction. It is known that many surfaces can catalyse this reaction. As an important step towards understanding the process, studies of oxygen chemisorption are essential. Recent theoretical studies of gas–surface interactions, primarily H_2 dissociative adsorption[1–5] and CO chemisorption[6–8] on different metal surfaces, have shown that state of the art *ab initio* calculations can provide a good description of potential energy surfaces and surface chemical bonds. In the present paper, we use a similar approach for oxygen adatoms chemisorbed on Pt{100}-(1×1).

As an oxidation catalyst, platinum is widely used in the chemical industry and is an important ingredient in automobile catalysts. The adsorption of oxygen on platinum single crystal surfaces, mostly on Pt{111} and {100}, has been studied experimentally using a variety of surface science techniques.[9] The Pt{111} surface is not significantly reconstructed, and chemisorbed oxygen forms overlayer *p*(2×2) and ($\sqrt{3}\times\sqrt{3}$)R30° structures, depending on coverage.[10] On the other hand, the clean Pt{100} surface is reconstructed to a stable phase in which the surface layer of platinum atoms has a quasi-hexagonal structure. The energy difference between the unrestructured and reconstructed phases has been measured as 0.21 eV/(1×1) Pt atom.[11] These two different structures exhibit very different chemical reactivities.[12] Experimental results showed the clean Pt{100}-(1×1) phase exhibits a bulk-terminated structure.[13–15] Oxygen adsorption is known to lift the surface reconstruction, but the detailed structure of oxygen on Pt{100} is not known. Norton *et al.* studied the interaction of O_2 with the (1×1)[16] and reconstructed hex surfaces.[17] At 123 K, O_2 does not dissociate on the reconstructed hex surface but adsorbs dissociatively on the (1×1) surface. Warming the surface to 240 K, a (2×1) oxygen overlayer is formed on the unreconstructed substrate. On further heating to ∼360 K, the surface transforms irreversibly to the oxygen stabilized (3×1) reconstructed phase. The (3×1) structure can also be formed by desorbing ∼0.2 ML oxygen adatoms from the oxygen saturated hex surface at higher temperature. Heating to desorb all the adsorbed oxygen leads to the reconstruction to the hex surface.

An earlier theoretical study of O/Pt{100} was performed by Bullett and Cohen[18] using a localized orbital method for a *c*(2×2) oxygen overlayer on a 3-layer Pt slab. From these calculations the strongest binding was found to occur at fourfold hollow sites, with the bridge site being the next and the atop the least stable. Benesh and Liyanage[19] calculated the electronic structure for *p*(1×1) oxygen on Pt{100} using a surface embedded Green function method by placing oxygen on the fourfold hollow site, and predicted that lower oxygen coverage would lead to a weakening of the O–Pt bond due to a reduction in the bonding–antibonding splitting. Our calculations contradict these two results. Firstly, we find that the most stable adsorption site for a *c*(2×2) oxygen adlayer on Pt{100}-(1×1) is the bridge site. Secondly, the calculated binding energies in the present study show an opposite tendency with decreasing oxygen coverage, as discussed below.

II. CALCULATIONS

Total energy pseudopotential calculations were performed within the framework of density functional theory

using a basis set consisting of plane waves. The surface is modeled using a slab inside a supercell. The electronic ground state of the system is directly located by a type of Car–Parrinello approach, the conjugate gradients minimization scheme. The total energy is calculated using CASTEP (Cambridge Serial Total Energy Package) code.[20] A Fermi surface smearing of 0.2 eV is employed and the energy extrapolated to zero temperature by the method of Gillan and De Vita.[21] *Ab initio* pseudopotentials in fully separable Kleinman–Bylander form[22] were generated by an improved kinetic-energy-filter optimization scheme.[23] The exchange and correlation energies are described in either the Ceperley–Alder form of local-density approximation (LDA)[24] or the Perdew–Wang form of the generalized gradient approximation (GGA).[25]

Previous calculations have shown that GGA calculations gave reliable descriptions of the total energy for chemisorption systems while the energies from LDA calculations show significant overbinding.[7,26] On the other hand, structures determined by GGA are usually no better than from LDA when compared to experimental results. Here we allowed the structure to be optimized with LDA and then used the self-consistent LDA density as an input for the GGA calculations.

The platinum and oxygen pseudopotentials have been tested both on bulk platinum and on the oxygen molecule. The LDA calculation with a 500 eV plane-wave cutoff gives a platinum lattice constant of 3.934 Å, in good agreement with the experimental value (3.92 Å). The calculated lattice parameter with GGA is 3.968 Å. For atomic and molecular oxygen, spin–polarization effects were included in the calculations. With a 500 eV cutoff, the calculations yield a bond length of 1.22 Å and dissociation energy of 5.73 eV; both are larger than the experimental values (1.207 Å and 5.127 eV[27]) but comparable with Becke's[28] calculations.

III. RESULTS AND DISCUSSION

A. Clean surface relaxation

The top-layer relaxation for Pt{100}-(1×1) has been calculated for a 4-layer Pt slab by fixing the lower layers at their bulk positions. The second layer Pt atoms were fixed at their bulk positions to avoid uncertainties caused by the finite size of the slab. The vacuum spacing between slabs is about 12 Å. Figure 1 shows the optimized structure. The top layer is relaxed towards the bulk, with the interlayer distance between the first and second layers decreased by 4.5%, from 1.967 Å of the calculated bulk value to 1.885 Å. The result in general agrees with experimental data;[13–15] the extent of top-layer relaxation is within experimental error. The energy difference between the unrelaxed and relaxed structures is rather small, about 30 meV/atom. The LDA surface energy for the bulk-terminated structure is 1.284 eV/(1×1) Pt atom, which is in reasonable agreement with the value of 1.21 eV/(1×1) Pt atom reported by Fiorentini *et al.*[29] using an all-electron full-potential linear muffin tin orbital method. On
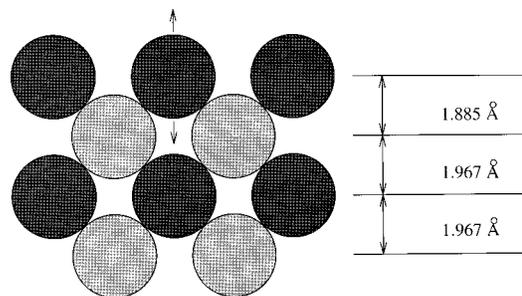

FIG. 1. LDA relaxed structure of the clean Pt{100}-(1×1) surface. Cut along ⟨010⟩ direction.

the other hand, the GGA energies with the LDA densities favor the bulk-terminated structure as compared with the LDA relaxed structure.

B. Atomic oxygen chemisorption

The disordered oxygen adatom overlayer formed on Pt{100}-(1×1) at 123 K transforms into a (2×1) structure after heating to ~240 K, which is believed to correspond to an overlayer on the unreconstructed surface. At higher annealing temperatures the surface is reconstructed, but to simplify the calculations, we ignore this complication here: A series of simple overlayer structures were examined. We note, however, that a study of the unreconstructed surface should provide some basis for understanding the driving force for the oxygen induced reconstructions. The bond strength between oxygen atom and surface was estimated in the following way. The total energy of atomic oxygen was calculated from the CASTEP code including spin–polarization. The adsorption energy per oxygen atom is

$$E_{ad} = \frac{1}{n} \left[E_{O,Pt} - (nE_O + E_{Pt}) \right], \tag{1}$$

where n is the number of oxygen atoms in the unit cell. $E_{O,Pt}$, E_O, and E_{Pt} represent the total energies of Pt slab with oxygen adatom(s), free oxygen atom and bare Pt slab, respectively. The heat of adsorption of O_2 is then

$$\Delta H_{ad} = D - 2E_{ad}, \tag{2}$$

where D is the dissociation energy of O_2.

1. c(2×2)-O/Pt{100}

The oxygen overlayer with this structure corresponds to a coverage of 0.5 ML. The total energies at this coverage for O adsorption on different high symmetry sites as shown in Fig. 2 are calculated. In Table I the binding energies of oxygen atoms on different sites are listed. In contrast to Bullett and Cohen,[18] our calculations show that the bridge site is energetically the most favorable site at this coverage. This result may seem very surprising; the fourfold hollow site was the favored candidate.

To check the validity of these results, the calculations were repeated by increasing the cutoff energy of the plane-wave basis set. We also checked our results using a 5-layer slab, placing O adatoms on both sides of the slab. The results
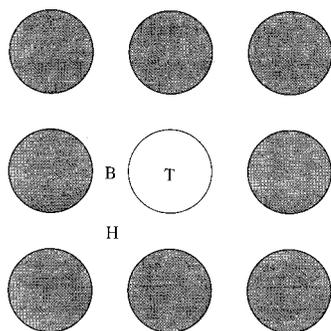
FIG. 2. Schematic view of the high symmetry sites of oxygen chemisorption on Pt{100}-(1×1). H—four-fold hollow site; B—bridge site; T—atop site.

of these calculations are summarized in Table II. These results confirm that at 0.5 monolayer coverage, the bridge site is energetically the most stable site. The differences for the GGA adsorption energies between bridge site and fourfold hollow site are bigger than found with LDA; this is in agreement with the observation that LDA tends to exaggerate the chemisorption energy at high coordination sites with respect to low coordination sites.[7]

For $p(2\times2)$ oxygen on Pt{111}, a LEED analysis showed that O atoms adsorb on fcc-hollow sites.[10] The O–Pt bond length was measured as 2.02 Å. A small lateral expansion of the triangle of the three Pt atoms directly below the O atom was observed. In the present calculations, the Pt surface atoms were constrained to relax only perpendicular to the surface. The fully relaxed O–Pt bond lengths for adsorption on the bridge and fourfold sites are different. The oxygen adatoms sits in the fourfold hollow site 1.05 Å above the first Pt layer, corresponding to an O–Pt bond length of 2.231 Å. The surface to second Pt interlayer spacing is simultaneously altered to 1.958 Å, close to the calculated bulk value. For O on the bridge sites, the forces exerted onto the two directly-bonded frozen Pt atoms are rather big at the minimum energy position, tending to push the two Pt atoms apart. In this case the O–Pt bond length was shortened to 1.940 Å and the metal interlayer spacing relaxed to 2.000 Å. With oxygen in the unstable atop site, the O–Pt bond length is further reduced to 1.789 Å, and here it tends to push the *surrounding* Pt atoms downward, causing the Pt atom directly underneath it not to stay in the same surface plane as the remaining surface atoms. The correlation between bond length and coordination of oxygen adatom to surface Pt atoms is as expected, and is in good agreement with general trends for oxygen on other metal surfaces.[30] This is readily explained

TABLE I. The LDA and GGA binding energies (in eV/O atom) for a $c(2\times2)$-O overlayer on Pt{100}-(1×1).

O site	E_{ad}		
	LDA relaxed	GGA	Ref. 18
Fourfold hollow	4.587	3.155	5.8
Bridge	5.129	3.809	5.2
Atop	3.920	2.860	3.8

TABLE II. Differences in GGA binding energies (in eV/O atom) between bridge and fourfold hollow sites for 0.5 ML O on Pt{100}-(1×1).

	$\Delta E_{ad}=E_{ad(hollow)}-E_{ad(bridge)}$
four layers, one side	−0.654
five layers, two sides	−0.635
four layers, one side, with 600 eV cutoff	−0.632

within effective medium theory; in order to provide the optimal electron density to form the chemisorption bond to fewer Pt atoms, the oxygen atom has to move closer to them.

Based on the calculated results, we can certainly rule out fourfold hollow sites for oxygen adatoms on unreconstructed Pt{100}−(1×1). The surface would restructure if the constraints imposed on the lateral movement in our calculations were removed, producing a lower energy structure. From experiments[16] it is known that there is an activation energy barrier associated with this process. The reconstruction could be modeled using the present approach, but due to its complexity and the computing costs, it was beyond our scope.

2. Oxygen–oxygen adatom interactions on Pt{100}-(1×1)

To study the interactions between O adatoms on the surface, we calculated the chemisorption energies at both lower and higher coverages. For a lower coverage, we chose a $p(2\times2)$ unit cell with one oxygen atom on one side of a four-layer Pt slab. This choice corresponds to an oxygen coverage of 0.25 ML. The calculations were performed for oxygen adatoms on both fourfold hollow and bridge sites. The chemisorption energy was also calculated for a full monolayer. In Table III we list the calculated chemisorption energies for these different coverages, including the energies at 0.5 ML. The calculated heats of adsorption are also shown, as obtained from Eq. (2) with D equal 7.271 and 5.728 eV for the LDA and GGA calculations, respectively. The results demonstrate a remarkable difference in the variation of bond energies or adsorption heats with coverage for the two sites, bridge and fourfold hollow. For the fourfold hollow sites the chemisorption energy decreases strongly with increasing oxygen coverage, indicating strong repulsive interactions between O adatoms on both nearest neighbor (nn) and next nearest neighbor (nnn) positions. Calculated as pairwise interaction energies, ω, the results yield $\omega_{nnn}=0.16$ eV and $\omega_{nn}=0.16$ eV, using the GGA values. In studying O chemisorption on Al{111}, Nørskov *et al.*[31] found that the finite size of the slab used in the calculation may contribute to the interaction energies, manifesting itself as a repulsive interaction. However, as shown by using a five-layer slab with O adatoms on both side of the slab, the finite size contribution to the repulsive interaction in the present calculation is small. In stark contrast with the results for the fourfold site, the binding energy at the bridge site does not show a significant difference for the two coverages, 0.25 and 0.5 monolayer, implying weak interactions between oxygen adatoms in nnn positions. This difference between the interac-

TABLE III. The LDA and GGA chemisorption energies (in eV/O atom) and heats of adsorption (in eV/O$_2$ molecule) for different oxygen coverages.

θ	O site	E_{ad}		ΔH_{ad}	
		LDA	GGA	LDA	GGA
1.0	fourfold hollow	4.144	2.524	1.017	−0.680
0.5	fourfold hollow	4.587	3.155	1.903	0.582
	bridge	5.129	3.809	2.987	1.890
0.25	fourfold hollow	5.584	3.798	3.897	1.868
	bridge	5.426	3.804	3.581	1.880

tion energies for bridge and hollow sites was investigated by analyzing the local chemical bonding, as discussed in the next section.

The calculated heats of dissociative chemisorption from LDA are comparable with calorimetric adsorption heats on Pt{100},[32] but the GGA values are considerably lower. However, a direct comparison with these experimental results is not meaningful, as there is evidence that substrate lattice reconstruction occurs with oxygen adsorption at 300 K. Rutherford backscattering measurements from both (3×1) and complex phases shows that a significant fraction (40–60%) of surface Pt atoms are displaced from their bulklike positions.[17] The displacements in both cases are greater than 0.25 Å; significant restructuring is incurred by oxygen chemisorption on Pt{100}-(1×1) at room temperature. However it is relevant to note that for the interaction of O$_2$ with Pt{111}, where no restructuring occurs, adsorption heat data are consistent with strong repulsive interactions between oxygen adatoms in threefold hollow sites; for third neighbor sites the pairwise interaction energy was found to be 0.21 eV,[33] in close agreement with our computed value of 0.16 eV for oxygen adatoms in fourfold sites on Pt{100}. Repulsive interactions between oxygen adatoms have also been inferred from a recent theoretical study of O adsorption on Ru{0001}.[34]

3. The chemisorption bond between oxygen and Pt{100}-(1×1)

In quantum chemistry the eigenstates of a system corresponds to specific molecular orbitals. These orbitals give substance to the chemical bonds formed in the molecule. Theoretically, the starting point of density functional theory is the total charge density, which determines the nature of the system. The formal physical meaning of the eigenvalues of the Kohn–Sham equation is not obvious. However, examining the charge density at each sampled Bloch state gives the corresponding characteristic molecular orbitals. This approach has been used widely in analyzing surface chemical bonds.[8,35–37] In our calculations the total charge density is obtained by sampling the surface Brillouin zone,

$$\rho_t(\mathbf{r}) = \sum_{k_j} \sum_{i_b} \rho_{k_j,i_b}(\mathbf{r}) = \sum_{k_j} \sum_{i_b} |\psi_{k_j,i_b}(\mathbf{r})|^2, \qquad (3)$$

where k_j and i_b are indices for k points and bands. The summation runs over all the sampled k points and occupied bands; $\psi_{k_j,i_b}(\mathbf{r})$ is a Bloch state which can be considered as an eigenstate of the periodic system. Note that $\rho_{k_j,i_b}(\mathbf{r})$ is the charge density at the corresponding Bloch state.

Figure 3 shows logarithmic total charge densities for O chemisorbed on fourfold hollow and bridge sites of Pt{100}−(1×1). We believe that considerably more information is obtained by examining symmetry and nodes in the charge densities of the sampled Bloch states. The charge densities of all sampled Bloch states, $\rho_{k_j,i_b}(\mathbf{r})$, have been plotted but only some of the states at the Γ point are shown in Fig. 4. The energy level of the oxygen 2s orbital is well below the Pt d-band. At this level, almost no metal character can be observed. With increasing energy, p_z-derived bonding states between adatoms and surface Pt atoms start to appear [Fig. 4(a)], and can be observed all the way to the top of the band [Fig. 4(e)]. Mixing between oxygen $p_{x(y)}$ orbitals with the d-band of Pt also spreads $p_{x(y)}$ character throughout the Pt d-band energy range. The p_z- and $p_{x(y)}$-derived features appear alternatively with increasing energy (Fig. 4). These results are consistent with the calculated local densities of states for oxygen on Pt{100}.[18] The bonding and antibonding interactions between oxygen p orbitals and Pt d orbitals can be clearly identified from these plots; antibonding states show nodes between the relevant atoms. Thus, the states show at 6.97 and 6.40 eV below E_F are bonding for O–Pt, whereas the states at 3.43 eV below and 0.01 eV above E_F are antibonding. Both σ and π bonding interactions contribute to the chemisorption bond. Direct interaction of the oxy-
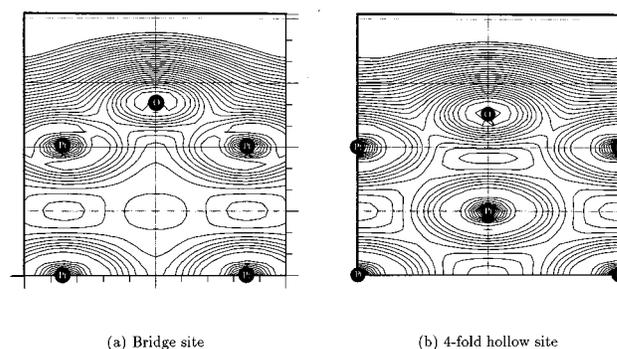

(a) Bridge site   (b) 4-fold hollow site

FIG. 3. Logarithmic total valence charge densities for oxygen chemisorbed on Pt{100}-(1×1). Cut along, (a) ⟨011⟩ direction and (b) ⟨010⟩ direction, through two directly bonded surface Pt atoms, and the O adatom, at a coverage of 0.5 ML.

(a) E_i-E_F = -6.97 eV

(b) E_i-E_F = -6.40 eV

(c) E_i-E_F = -6.39 eV

(d) E_i-E_F = -3.43 eV
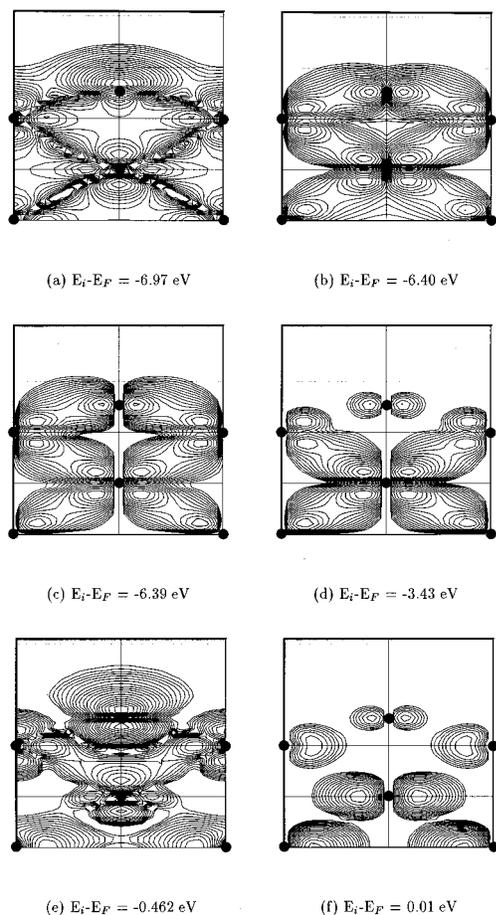
(e) E_i-E_F = -0.462 eV

(f) E_i-E_F = 0.01 eV

FIG. 4. Logarithmic partial charge density contour plots at $\overline{\Gamma}$ for oxygen chemisorbed on the hollow site of Pt{100}-(1×1), at the energies shown, at 0.5 ML. Cut along the ⟨010⟩ direction, through two directly bonded surface Pt atoms. The black dots show the atomic centers.

(a) Bridge site, E_i-E_F = -5.95 eV

(b) Bridge site, E_i-E_F = -5.78 eV

(c) 4-fold site, E_i-E_F = -5.68 eV

(d) 4-fold site, E_i-E_F = -5.64 eV

FIG. 5. Logarithmic charge density contour plots at $\overline{\Gamma}$ for oxygen chemisorbed on Pt{100}-(1×1) at 0.5 ML, cut through the oxygen atom center parallel to the surface. The black dots show the projected center of Pt atoms in the surface plane.

gen p-orbitals with second layer Pt atoms can also be observed.

Figure 5 shows the partial charge densities at 5.95, 5.78 and 5.68, 5.64 eV below E_F for oxygen on bridge and fourfold hollow sites, respectively, cutting through the oxygen plane parallel to the surface. Figures 5(a) and 5(b) show that for the bridge site the bonding between O adatoms and surface Pt atoms is localized to the two bridging Pt atoms. The $p_{x(y)}$-like orbitals of oxygen are aligned along the direction of the bridging atoms. This "local structure" generates little or no overlap with neighboring oxygen adatoms as the coverage is increased from 0.25 to 0.5 MI, in keeping with the observation that the bonding energy is unaltered. However, when the oxygen atoms are moved to fourfold hollow sites as shown in Figs. 5(c) and 5(d), the $p_{x(y)}$-like orbitals spread towards the four Pt atoms, and are considerably less localized. In this case, the "local structure" involves four top layer Pt atoms. On increasing the coverage from 0.25 to 0.5 MI, strong overlap between these "local structures" occurs; each Pt atom is then bonded to two oxygen atoms. Since these are filled states, Pauli repulsion between the mixed states formed from the oxygen p_x and p_y orbital states is large, and we conclude that this repulsion is largely respon-
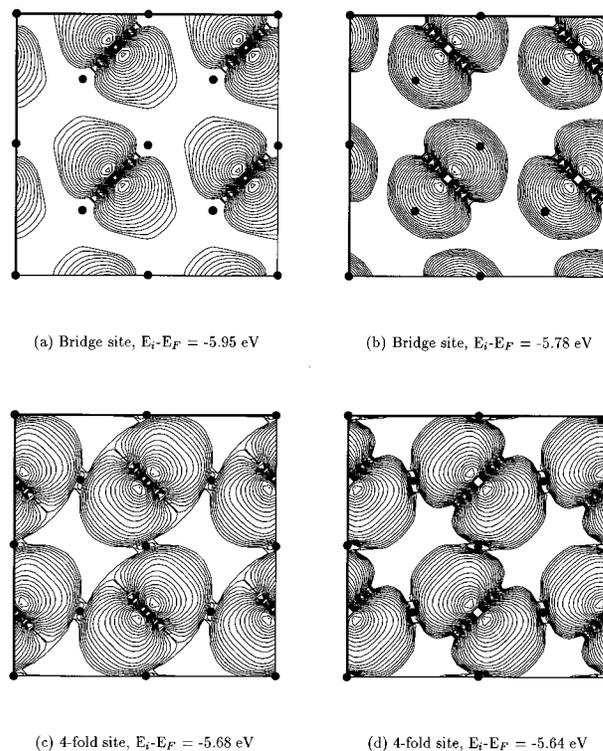
sible for the significant fall in bond energy with coverage when oxygen is adsorbed in the high symmetry fourfold hollow site. The structures shown in Fig. 5, which appear in the sampled Bloch states, are typical for the interactions involving oxygen $p_{x(y)}$ orbitals. For oxygen on bridge sites, the p_x and p_y orbitals are not equivalent; p_x interacts with the two bridging Pt atoms in the top layer while p_y interacts with the Pt atoms in the second layer. The larger separation between oxygen atoms and second layer Pt atoms prevents p_y orbitals from mixing with Pt d orbitals to the same extent as the p_x. For oxygen on the fourfold hollow, the p_x and p_y orbitals are equivalent. However, the loss of symmetry in the slab with four layers gives rise to some nondegeneracy in the p_x and p_y orbitals with a splitting of less than 0.05 eV.

Comparison of the present data (Table I) with the earlier localized orbital calculations of Bullett and Cohen[18] for oxygen on bridge site shows good comparability with the LDA results. The localized orbital approach can therefore give a reasonable description of localized bonding between oxygen and surface Pt atoms, but fails to account for the Pt-mediated oxygen–oxygen interactions, which is why the binding energy for oxygen on fourfold sites at 0.5 ML coverage was too strong.

IV. CONCLUSIONS

The novel result from the present work is the remarkable dependence of lateral interactions between adatoms at a sur-

face on site symmetry. For oxygen adatoms on bridge sites, the bond energy to the surface is the same at 0.25 and 0.5 ML, indicating no net interaction between adatoms at this spacing, but on the fourfold hollow sites the adatoms are strongly destabilized as the coverage is increased over this range, consistent with a next nearest-neighbor pairwise repulsive interaction energy of 0.16 eV. At 0.25 ML the two sites are almost equally stable, with a bond energies to the surface of 3.8 eV/O atom. It is worth noting that adatoms in fourfold sites are involved in bond-sharing to surface layer Pt atoms at all coverages above 0.25 ML, whereas for bridged oxygen atoms bond-sharing with surface Pt atoms is avoided up to 0.5 ML. This is one level of explanation for the present result. However, an analysis of the charge densities of the oxygen atom p_x- and p_y-derived Bloch states for adatoms in the two sites clearly demonstrates that in the fourfold sites these states are considerably less localized. The overlap between next nearest-neighbor sites in the $c(2\times2)$ overlayer structure is significant, and, since these are filled states, Pauli repulsion is large, and we conclude that it is this repulsion which leads to the strong fall in bond energy with coverage in fourfold sites. Conversely, the spatially more compact mixed $p_{x(y)}$ states formed in the bridge sites show no significant overlap in the next nearest-neighbor bridging positions. In both cases, mixing between oxygen p-orbitals and the Pt d states is observed over the whole d-band energy range. The atop site is found to be considerably less stable than bridge or fourfold site for oxygen adatom chemisorption at 0.5 ML.

The binding energy for oxygen adatoms at bridge and fourfold sites is almost identical, at 3.8 eV, at a coverage of 0.25 ML, implying not only no site preference at this coverage, but also a very low barrier for oxygen adatom diffusion on the unreconstructed Pt{100}−(1×1) surface. However, at 0.5 ML there is a significant binding energy difference between these two sites, of ~0.6 eV, and we conclude that this is a measure of the diffusion barrier at this coverage.

ACKNOWLEDGMENTS

[1] B. Hammer, K. W. Jacobsen, and J. K. Nørskov, Phys. Rev. Lett. **69**, 1971 (1992).
[2] J. A. White and D. M. Bird, Chem. Phys. Lett. **213**, 422 (1993).
[3] B. Hammer, M. Scheffler, K. W. Jacobsen, and J. K. Nørskov, Phys. Rev. Lett. **73**, 1400 (1994).
[4] J. A. White, D. M. Bird, M. C. Payne, and I. Stich, Phys. Rev. Lett. **73**, 1404 (1994).
[5] J. A. White, D. M. Bird, and M. C. Payne, Phys. Rev. B **53**, 1667 (1996).
[6] B. Hammer, Y. Morikawa, and J. K. Nørskov, Phys. Rev. Lett. **76**, 2141 (1996).
[7] P. Hu, D. A. King, S. Crampin, M.-H. Lee, and M. C. Payne, Chem. Phys. Lett. **230**, 501 (1994).
[8] P. Hu, D. A. King, M.-H. Lee, and M. C. Payne, Chem. Phys. Lett. **246**, 73 (1995).
[9] See for example, A. A. Luntz, M. D. Williams, and D. S. Bethune, J. Chem. Phys. **89**, 4381 (1988), and reference therein for Pt{111}; and J. M. Bradley, X.-C. Guo, A. Hopkinson, and D. A. King, J. Chem. Phys. **104**, 4283 (1996), and reference therein for Pt{100}.
[10] N. Materer, U. Starke, A. Barbieri, R. Döll, K. Heinz, M. A. Van Hove, and G. A. Somorjai, Surf. Sci. **325**, 207 (1995).
[11] Y. Y. Yeo, C. E. Wartnaby, and D. A. King, Science **268**, 1731 (1995).
[12] J. M. Bradley, A. Hopkinson, and D. A. King, J. Chem. Phys. **99**, 17032 (1995).
[13] R. Feder, Surf. Sci. **68**, 229 (1977).
[14] J. A. Davies, T. E. Jackman, D. P. Jackson, and P. R. Norton, Surf. Sci. **109**, 20 (1981).
[15] E. Lang, W. Grimm, and K. Heinz, Surf. Sci. **117**, 169 (1982).
[16] P. R. Norton, P. E. Binder, and K. Griffiths, J. Vac. Sci. Technol. A **2**, 1028 (1984).
[17] K. Griffiths, T. E. Jackman, J. A. Davies, and P. R. Norton, Surf. Sci. **138**, 113 (1984); P. R. Norton, K. Griffiths, and P. E. Bindner, *ibid*. **138**, 125 (1984).
[18] D. W. Bullett and M. L. Cohen, J. Phys. C **10**, 2101 (1977).
[19] G. A. Benesh and L. S. G. Liyanage, Surf. Sci. **261**, 207 (1992).
[20] M. C. Payne, M. P. Teter, D. C. Allen, T. A. Arias, and J. D. Joannopoulos, Rev. Mod. Phys. **64**, 1045 (1992).
[21] A. De Vita and M. J. Gillan, J. Phys.: Condens. Matter **1**, 6225 (1991).
[22] L. Kleinman and D. M. Bylander, Phys. Rev. Lett. **48**, 1425 (1982).
[23] M.-H. Lee, Ph.D. thesis, Cambridge University, 1995; J.-S. Lin, A. Qteish, M. C. Payne, and V. Heine, Phys. Rev. B **47**, 4174 (1993); A. Rappe, K. Rabe, E. Kaxiras, and J. D. Joannopoulos, Phys. Rev. B **41**, 1227 (1990).
[24] D. M. Ceperley and B. J. Alder, Phys. Rev. Lett. **45**, 566 (1980); J. P. Perdew and A. Zunder, Phys. Rev. B **23**, 5048 (1981).
[25] J. P. Perdew, J. A. Chevary, S. H. Vosko, K. A. Jackson, M. R. Pederson, D. J. Singh, and C. Fiolhhais, Phys. Rev. B **46**, 6671 (1992).
[26] B. Hammer, K. W. Jacobsen, and J. K. Nørskov, Phys. Rev. Lett. **70**, 3971 (1993).
[27] D. R. Lide, *CRC Handbook of Chemistry and Physics*, 75th ed. (CRC, Boca Raton, FL, 1995).
[28] A. D. Becke, J. Chem. Phys. **97**, 9173 (1992).
[29] V. Fiorentini, M. Methfessel, and M. Scheffler, Phys. Rev. Lett. **71**, 1051 (1993).
[30] F. Besenbacher and J. K. Nørskov, Prog. Surf. Sci. **44**, 5 (1993).
[31] J. Jacobsen, B. Hammer, K. W. Jacobsen, and J. K. Nørskov, Phys. Rev. B **52**, 14954 (1995).
[32] Y. Y. Yeo, L. Vattuone, and D. A. King (to be published).
[33] Y. Y. Yeo, L. Vattuone, and D. A. King, J. Chem. Phys. **104**, 8096 (1996).
[34] C. Stampfl and M. Scheffler, Phys. Rev. B **54**, 2868 (1996).
[35] D.-S. Wang, A. J. Freeman, and H. K. Krakauer, Phys. Rev. B **24**, 3092 (1981).
[36] E. Wimmer, C. Fu, and A. J. Freeman, Phys. Rev. Lett. **55**, 2618 (1985).
[37] H. Ishida and K. Terakura, Phys. Rev. B **40**, 11519 (1989).